ORIGINAL ARTICLE

Influence of non-conventional beam profile on edge effects in laser forming of AISI 304 stainless steel plate

E. R. Imam Fauzi [1] · M. S. C. Jamil [2] · Z. Samad [1] · M. A. Sheikh [3] · A. M. Najib [4]

Abstract

Laser forming is an innovative technique that uses a defocused laser beam to form sheet metal by thermal stresses rather than external forces. This offers excellent and promising potential applications in rapid prototyping, straightening, aligning, and adjusting of macro/micrometallic components. However, the undesirable edge effects in laser forming reflect that the bending angle is not constant along the scanning line. This paper presents an analytical study of edge effects in laser bending of AISI 304 stainless steel plate. Experimental and numerical investigations aimed at understanding the effects of the triangular beam geometry with different aspect ratios were clearly demonstrated. A validated thermal model was developed, and different sets of FE simulations were carried out by varying heat input values and aspect ratio of laser beam with constant scanning speed. It is evident that triangular beam with highest aspect ratio was preferable to produce a higher bending angle with lesser edge effect at higher power intensity. It is found that triangular beam geometries are more effective in minimizing the bending angle variation compared with the circular beam.

Keywords Laser forming · Edge effect · Finite element · Stainless steel

1 Introduction

Laser forming is a newly developed technique, which offers many advantages to many relevant industry sectors including automotive, ship building, aerospace, and microelectronics. In spite of using any conventional die and press, the utilization of thermal stresses to deform structural elements provides a fast and precise control without any significant microstructural changes of material involved. The non-contact nature of the process that makes it independent of tool inaccuracies has the

ability in controlling more accurate energy source and practical for remote application purposes.

Despite the mentioned advantages, some major limitations need to be addressed before laser forming becomes a practical technology. One of the existing issues is the geometric irregularities along the bending angle, or the edge effects phenomenon. During straight line bending, the bending angle shows variation along the scanning path such that the angle near the exit edge is generally larger than that near the entrance edge. This has caused the development of curves on the edge of the sheet. The edge effects are obviously undesirable since they cause the deviation from the design intent (constant bending angle along the straight bending edge), cause a certain warpage of the component, and may cause additional residual stresses.

Previous researchers have proposed several causes of the edge effect, namely, bend angle [1], laser scanning speed [2, 3], laser beam diameter [4], assistant force effect [5–7], and cooling rate [8]. Jha et al. [1] explored the phenomena of multi-curvature bend angles along a single laser scan path with different scanning speeds, number of passes, and input power. Their results showed that a single laser scan path could sometimes yield to multi-curved bends. To minimize edge effect, Shen et al. [2] proposed a method of varying the laser scanning speed along the scan path. Slow scanning speed is

✉ E. R. Imam Fauzi
elfirahayu2006@yahoo.com

1 Manufacturing Engineering Group, School of Mechanical Engineering, Universiti Sains Malaysia (USM), 14300 Nibong Tebal, Penang, Malaysia

2 Dscaff Group, Mont Kiara, Kuala Lumpur, Malaysia

3 Laser Processing Research Centre (LPRC), School of Mechanical, Aerospace and Civil Engineering, University of Manchester, M60 1QD, Manchester, UK

4 Fakulti Kejuruteraan Pembuatan, Universiti Teknikal Malaysia Melaka (UTeM), Hang Tuah Jaya, 76100 Durian Tunggal, Melaka, Malaysia

used at the entrance and exit edges which enhance the yielding to achieve uniform bending angle along the bending edge. Hu et al. [4] have conducted experimental tests on edge effects in laser bending. The beam diameter was found to have the most significant processing parameter, and a combination of the laser power and scanning velocity provided the highest interaction effect. A work by Safdar et al. [3] demonstrated that the variation of scanning speed could counter the effect of varying mechanical resistance along the bending edge and hence minimize the edge effects. Birnbaum et al. [5] studied the effect of clamping the sheet on the bending angle profile. They have found that in a constrained sheet, due to the comparative displacement of the free edge of the sheet, variations in the bending angle are increased. Hu et al. [6] investigated the methods of reducing the edge effect by changing the constraint conditions. It was found that the deviation of the bending angle along the scanning path was reduced significantly. However, the bending angles of the two ends were larger than those in the middle. Shi et al. [7] proposed a method to improve the forming accuracy by using two unequal concentrated forces at the entering and exiting end. Interestingly, from the results, the relative variation value of the bending angle decreases by almost 80% as compared with that of pure laser forming.

Alternatively, beam geometry can be utilized to minimize the edge effect characteristics significantly. Up to author's knowledge, limited information is available about the effect of different beam geometries on laser bending. A few authors [9, 10] have indirectly discussed the use of rectangular and elliptical beams when investigating laser forming using diode laser. However, the discussion is limited to the effect of beam orientation on the bending angle of the deformed plates. Additionally, the heat distribution analysis of a non-conventional laser beam profile such as doughnut profile was investigated numerically in [11, 12]. No discussion is offered to explain the cause of such effect. Safdar [13] studied the effect of beam geometries on various laser processes such as laser transformation hardening, laser surface heating, and laser melting. Nevertheless, his research in laser forming was limited to tube bending. Irawan [14] investigated the effects of various different beam geometries including diamond transverse, triangular, circular, and rectangle on the edge effect phenomenon. It is evident that beam geometry has influence on the bend angle variation along the scanning path. As the result, it is found that triangular beam has a promising potential to produce high bend angle with small variation of edge effects. This finding is supported by the study done by Jamil [15], which agreed that the beams with a narrow leading edge are preferable to produce less bending angle variations compared with the ones with wider leading edge.

This paper presents an experimental and numerical analysis of the effects of triangular beam geometry with various aspect ratios on edge effect characteristics during laser bending of AISI 304 stainless steel. The numerical investigation of the

edge effects was successfully demonstrated by varying laser power at a constant scanning speed. A commercial finite element analysis software package ANSYS® was used in thermal and structural analysis. The experimental validated simulation model results were analyzed to provide more insights into the causes of the edge effects.

2 Experimental procedure

Experiments were carried out with a Laserline LDL 160–1500 diode laser as shown in Fig. 1. The laser operates at a wavelength of 808–904 nm and has a max power output of 1.5 kW. The raw beam of the laser is a rectangular profile with a Gaussian intensity distribution. The laser was coupled to a 1-mm-diameter fibre optic cable and a 1:1 optical imaging system with a focal length of 85 mm. This produced a circular beam with a 'top-hat' (approximately uniform) intensity distribution. However, the efficiency of the laser was reduced to 72% due to the fibre coupling. The beam was tested at laser powers of 400 W, 600 W, and 800 W with a laser beam traverse speed of 10 mm/s. The materials used in the experiments were assumed to be homogenous and isotropic. The plates used were 110 mm in length, 50 mm in width, and 2 mm in thickness. Ten millimeters of the edge length of the plate was clamped down at one end. The clamp was mounted on a CNC table controlled by a CNC Automation Controller C116-4isel. The CNC table was used to move the plate under the beam at the desired velocity. The plate material used was AISI 304 stainless steel which is an austenitic low carbon steel. The material composition of AISI 304 is shown in Table 1.

2.1 FE model development

In laser bending of plates, only heating load is being transferred onto the plate by the laser beam. This heat is transferred mainly by mean of conduction, while some of it is lost to surroundings due to convection and radiation. Heat losses due to radiation, however, were negligible. In general, the temperature distributions in plate can be calculated using the basic formulation of transient heat transfer as follows:

$$-\left(\frac{\partial q_x}{\partial x} + \frac{\partial q_y}{\partial y} + \frac{\partial q_z}{\partial z}\right) + Q = \rho c \frac{dT}{dt} \quad (1)$$

where q_x, q_y, and q_z are the components of heat flow through the unit area, T is temperature, ρ is material density, c is specific heat capacity, t is time, and Q is heat source (expressed as heat generation per unit volume). ρ and c are temperature-dependent properties. According to Fourier's law, the thermal gradient components for three dimensional heat flow can be written as follows:

Fig. 1 Schematic diagram of the experimental setup
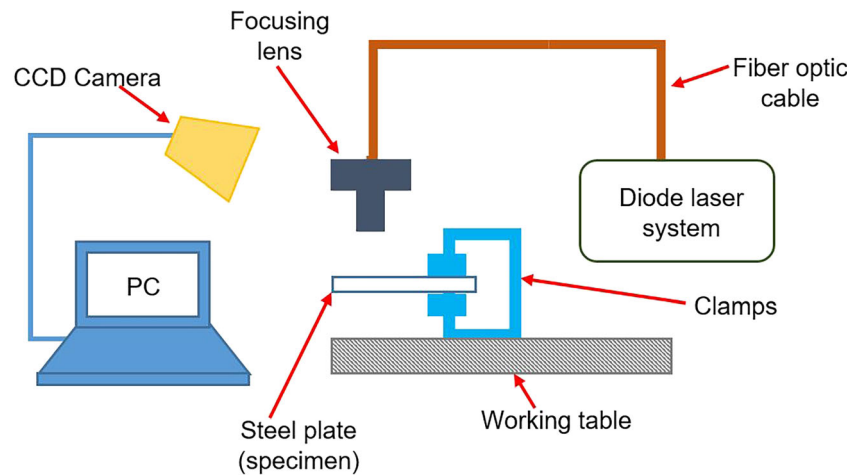
$$q_i = -k \frac{\partial T}{\partial i} \tag{2}$$

where k is the thermal conductivity of material. Substitution of Eq. (2) into Eq. (1) gives the following relations:

$$\frac{\partial}{\partial x}\left(k\frac{\partial T}{\partial x}\right) + \frac{\partial}{\partial y}\left(k\frac{\partial T}{\partial y}\right) + \frac{\partial}{\partial z}\left(k\frac{\partial T}{\partial z}\right) + Q = pc\frac{\partial T}{\partial t} \tag{3}$$

For interpolation of temperature inside a finite element, shape function N_i was used. By using the Galerkin method and differentiation of the temperature-interpolation equations, the basic heat transfer equation can be rewritten into the following form:

$$\int_V \left(\frac{\partial q_x}{\partial x} + \frac{\partial q_y}{\partial y} + \frac{\partial q_z}{\partial z} - Q + pc\frac{\partial T}{\partial t}\right) N_i dV = 0 \tag{4}$$

The nonlinear transient dynamic structural equation for finite element is expressed in the following matrix form:

$$[K(T)]\{u(t)\} = \{F^{th}(t)\} \tag{5}$$

where $[K(T)]$ is temperature-dependent stiffness matrix, $\{F^{th}(t)\}$ is thermal load vector, and $\{u(t)\}$ is nodal displacement vector. The thermal load vector, $\{F^{th}(t)\}$, can be calculated for plane strain as follows:

$$\{F^{th}(t)\} = \int_{Vol} [B]^T \frac{E\overline{\alpha}(T)\Delta T}{1-2v} \delta dV \tag{6}$$

where $[B]$ is the strain displacement matrix, E is the elastic modulus, v is Poisson's ratio, ΔT is the temperature difference, and δ is the matrix $[1\ 1\ 1\ 0\ 0\ 0]^T$. Total strain can be evaluated from nodal displacements by using:

$$\{\varepsilon\} = [B]\{u\} \tag{7}$$

where $\{u\}$ is the nodal displacement vector. The total strain for the plate subjected to the thermal load consists of thermal, plastic, and elastic strain components:

$$\{\varepsilon\} = \{\varepsilon^{th}\} + \{\varepsilon^{pl}\} + \{\varepsilon^{el}\} \tag{8}$$

where $\{\varepsilon^{th}\}$ is thermal strain vector, $\{\varepsilon^{pl}\}$ is plastic strain vector, and $\{\varepsilon^{el}\}$ is elastic strain vector.

In the laser forming process simulation, the laser beam is treated as a moving face flux. A commercial software package ANSYS Parametric Design Language (APDL) was used to simulate all processes. Structured grid approach was applied in creating the mesh model for this study. Nodes were placed in a grid form as to represent the whole area of the beam. A surface heat flux is then applied on the external faces of a group of hexahedral elements (six faces to form brick-like elements). In order to reduce computational time while ensuring accurate simulation results, the plate model was divided into three volumes, where a higher density mesh with fine hexahedral pattern was created in the scanning region, free tetrahedral meshes were used in the neighbouring zone, and lastly, coarse meshes were used in the region further away from the scanning path.

For the thermal analysis, ANSYS®-type Solid70 was used due to its thermal conduction capability, whereas ANSYS®-type Solid185 was used in structural analysis since each element has the capability of plasticity, deflection, and strain. The localization of the laser heat flux around the heating region allows the bending

Table 1 Material composition of AISI 304 stainless steel [15]

Material	wt%
Cr	18–20
Ni	10.5
C	0.08
Mn	2
Si	0.75
P	0.045
S	0.03
N	0.1

process to be simplified into half plate model with symmetric boundary conditions. The temperature dependency of material properties for the plate such as its thermal conductivity, specific heat, thermal expansion coefficient, Poisson's ratio, elastic modulus, yield stress, and density has been incorporated to the model [16]. Basic assumptions of the model were made as follows:

i.   Material is homogenous and isotropic.
ii.   Laser intensity distribution is assumed to be uniform and operates in a continuous-wave mode.
iii. Bauschinger's effect is neglected.
iv.   The von Mises criterion has been used for plastic yielding.
v.   Energy dissipation due to plastic deformation is neglected when compared with energy involved in the thermal process
vi.   All exposed surfaces of the plate were subjected to convection but radiation was ignored.

In this present study, the beam was simulated as a single scan across the plate. Six different beam geometries as shown in Fig. 2 were selected for preliminary investigation. A circular beam has been included in the study to provide the benchmark for conventional laser forming process.

The area of each beam was designed to be approximately 19.64 mm² regardless of geometry. This ensured the same power intensity was maintained across all beams and an equivalent amount of energy was transferred to the plate. With the area constant for each beam, the amount of nodes was also approximately equal. Each mesh in the laser-irradiated beam was 0.0625 mm²; therefore, each beam was created to contain 156 meshes whenever possible. For preliminary study, all six beam geometries were simulated at a velocity of 10 mm/s and at a power of 400 W. Out of the six beam geometries simulated, the diamond transverse beam produced the highest bending angle with a very high degree of angle variation, whereas the triangular beam offered almost the same results with less angle variation. From these results, triangular beam was further investigated by conducting additional simulations at varying aspect ratios. Six different aspect ratios of triangular beam as shown in Table 2 were simulated and analyzed. All sets were tested under varying a laser power of 400 W, 600 W, and 800 W and at constant speed of 10 mm/s.

2.2 Model validation

To validate the numerical model, the numerical results of bending angle variation have been compared with the experimental results as illustrated in Fig. 3. The bending angle variation which is defined as the difference between the maximum and minimum bending angles along the scanning line, were calculated and plotted at different laser power. It is evident that the simulation results were well correlated with the experimental data. The difference between experimental data and simulation results is a little greater at the highest laser power (800 W), in which the difference is about 7.14%. This small discrepancy between the numerical and experimental data is mainly due to the inaccurate mechanical properties of the material at high temperature.

3 Results and discussion

3.1 Effect of beam geometry and aspect ratio

The edge effect in laser bending is contributed by several simultaneously occurring factors including material constraint for bending and the relative difference in contraction of the top and the bottom surfaces along longitudinal direction. The dependency of beam geometry and peak temperature on bending angle has been presented in this study. For the preliminary study, the laser bending process was simulated with six different beam geometries at a laser traverse speed of 10 mm/s and a laser power of 400 W. The simulated results were summarized in Table 3. The diamond transverse beam was found to produce the highest bending angle followed by triangle beam, whereas the rectangle beam produced the lowest bend angle.

Figure 4 shows that a general trend exists between the maximum temperatures reached in the plate and the resulting bend angle. The trend shows that the peak temperature inversely affects the bend angle. This temperature effect is due to the temperature gradient mechanism that occurs to form the bend. When the plate surface is irradiated with the laser beam, the layers at the top surface of the plate are at higher temperatures than the bottom surface layers. This allows the top plate layers to plastically deform more. After the laser scan is complete, the plate is rapidly cooled which causes thermal
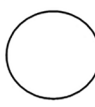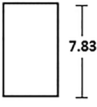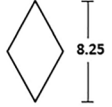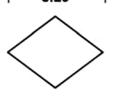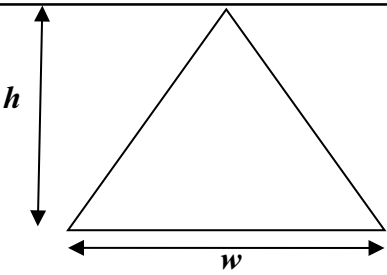
	Circular	Rectangle	Triangle	House	Diamond	Diamond Transverse
Beam Profile	5	2.51 / 7.83	5.83 / 6.73	3.18 / 6.64 / 4	4.76 / 8.25	8.25 / 4.76
Aspect Ratio	1	0.32	1.15	0.60	0.58	1.73

Fig. 2 Six beam geometries with similar effective areas

Table 2 The dimension of triangular beam geometry for FE simulation

Total area of beam = 19.64mm^2

Aspect ratio $= \dfrac{w}{h}$

Set	1	2	3	4	5	6
Height, h (mm)	7.30	6.80	6.43	6.12	5.83	5.60
Width, w (mm)	5.45	5.78	6.11	6.42	6.73	7.00
Aspect ratio	0.75	0.85	0.95	1.05	1.15	1.25

contraction. This results in the plate to bend towards the laser beam. From the results, it is seen that the beams with a longer dimension in the scanning direction with respect to its lateral dimension generate higher temperatures despite the fact that the power intensity and the beam effective area are similar for all cases. This occurs due to the duration of interaction between beam and material during the irradiation period. The duration of the beam-material interaction can be expressed as:

$$t_s = {d_{ax}}/{v} \tag{9}$$

where d_{ax} is the ratio of the axial length and v is the scanning speed. In this case, the rectangular beam which has the longest axial length produces the highest temperature of 685 °C, followed closely by diamond beam which gives almost the same temperatures (680 °C).

Aspect ratio of the beam influences the edge effect characteristics. The tendency for the scanning line to curve away from its original position increases as the beam axial length increases [10]. As evident from Fig. 5, aspect ratio significantly impresses the bending angle formation. It could be seen that the bending angle increases with the increase of aspect ratio.
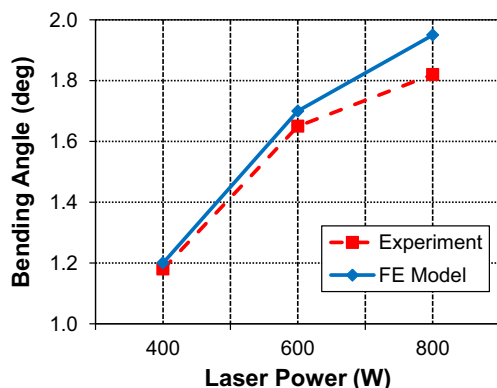
Fig. 3 Comparison of bending angle variation between experimental results and FE model using circular beam (irradiation area = 19.64 mm^2) at constant speed of 10 mm/s

The diamond transverse beam which possessed the highest aspect ratio of 1.73, gives the highest bend angle of 1.31°. The triangular beam with 1.15 aspect ratio gives a bend angle of 1.21°, whereas the conventional circular beam produces a slightly lower value of bend angle at 1.16°. This indicates that widening the beam geometry has a more impact on the bending angle than lengthening it.

The undesirable variation of bending angle along the bending edge has been found in all samples. All six beam geometries used here were producing varying degrees of edge effects as illustrated in Fig. 6. The percentage variation is measured with respect to the bending angle at the beam entrance and can be used to describe the edge effect for each beam. It is evident that bending angle at the beam exit is higher than at the entrance for all beam geometries. This is mainly due to the inherent asymmetry of the process, in that the heat imparted into the plate as the laser beam transverses across it. The heat is continually flowing into the cold region ahead of the beam. Due to this phenomenon, the plate equilibrium conditions with stable peak temperature were realized at the centre of the plate. However, as the beam reaches the exit edge, the heat flowing ahead of the beam cannot travel any further and so a heat buildup occurs. Thus, the exit edge experienced a higher peak temperature as compared with the centre region. This non-uniform temperature distribution can be attributed to the bending angle variation. This follows the general finding found by previous researchers [15, 17–19].

Table 3 Result of bending angle for different beam geometries

Beam geometry	Bend angle (°)
Diamond transverse	1.31
Triangle	1.21
Circle	1.16
House	0.99
Diamond	0.85
Rectangle	0.56
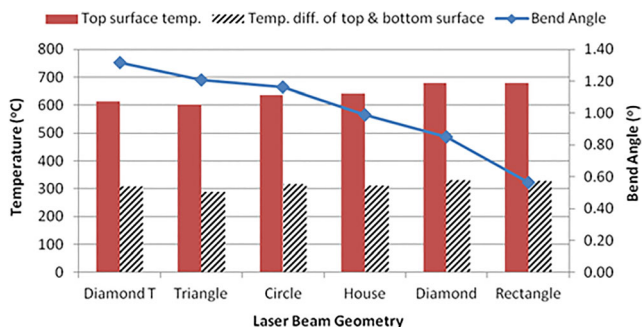
Fig. 4 Effect of temperature on bend angle for different beam geometries

Fig. 6 Bend angle variation along scan path for six beam geometries

Figure 7 shows the maximum and average bend angle variation compared with the bend angle for each of the six beams. The figure shows a trend that high bend angle results in high degree of variation with the exception of the triangular beam. The diamond transverse beam was found to produce the highest bending angle followed by triangular beam. In terms of bend angle variation, the triangular beam offered the best result of generating the less angle variation compared with diamond transverse beam. This leads to the conclusion that the triangular beam geometry is the better option for lower edge effects.

Figure 8 proves that the aspect ratio of the beam geometry has an influence on the resulting bend angle. It is observed that a higher bending angle could be achieved by increasing the aspect ratio and laser power. However, there is a threshold value of the aspect ratio to bend further. As seen from the result, aspect ratio from 0.75 to 0.95 gives a higher value of increment in bending value compared with aspect ratio from 1.05 to 1.25. A slight increment of the bend angle can be observed as the aspect ratio builds up. However, at a laser power of 400 W, a threshold value was found at an aspect ratio of 1.05. From this point onwards, the bending angle variation started to level off. This indicates that there is a threshold value, where the increment in the bending angle starts to level off. For the case of 600 W laser power, the variation is quite uniform, whereas for the case of higher laser power (800 W), a gradually decrement of angle variation was present as the aspect ratio increases. In the case of the conventional circular beam, the bending angle variation is much
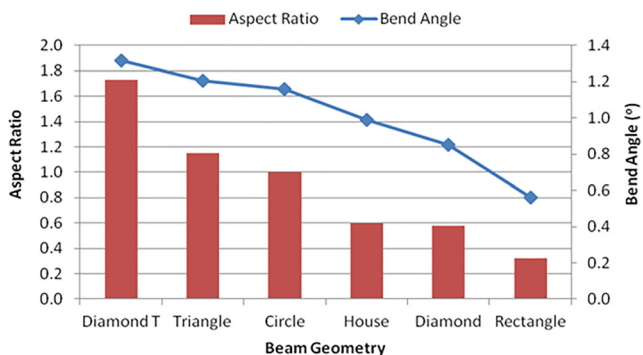
higher compared with triangular beam at any intensity levels. It is obvious that triangular beams are more effective in minimizing the bending angle variation compared with the circular beam. Thus, the edge effect can be reduced as well by using triangular laser beam in laser forming process.

3.2 Plastic deformation analysis

Figure 9 shows the plastic deformation from the laser irradiation of the top and bottom half of the plate thickness and its effect on bend angle at different values of laser power. All beams produce a higher plastic deformation in the top half of the plate which accounts for about 70–74% of the total plastic deformation throughout the thickness. It can be seen that circular beam produces the highest sum of plastic deformation at all laser power ranges. Despite having the largest plastic deformation, the bending angle obtained can be superseded by triangular beam with a higher aspect ratio. This shows that large plastic deformation across the thickness does not necessarily produces high bending angle. This is because any plastic strains below the neutral axis create counter bending on the plate. To explain this, if an equal area of plastic strain is distributed below and above the neutral axis, then, the plate will undergo upsetting mechanism and in theory, no bending angle will be produced. From the results, it is evident that there is a direct correlation between the variations of plastic deformation (between top and bottom halves of the plate) and the magnitude of bending angle. It can be seen that the top
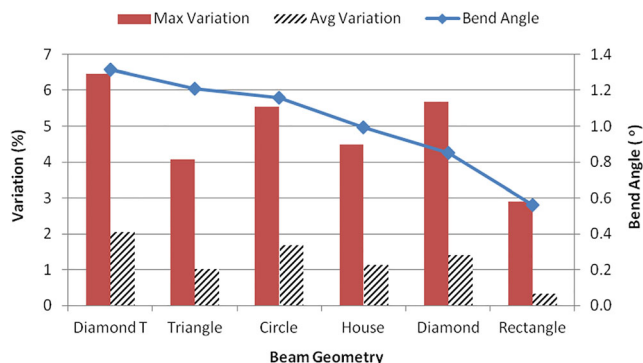

Fig. 5 Effect of aspect ratio on bend angle for different beam geometries

Fig. 7 Maximum bend angle variation and average bend angle variation for all beam geometries
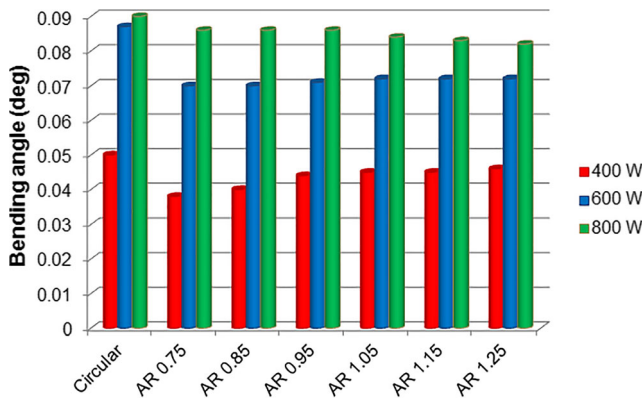
Fig. 8 Bending angle formation of different aspect ratios under varying laser power for triangular beam profile

half deformation is much higher compared with the bottom half deformation. This is due to the top half area is closer to the scanning laser irradiation. The larger the difference between top half and bottom half deformations, the higher bending value is obtained. In this case, triangular beam which possesses 1.25 aspect ratio is the optimum beam which produces
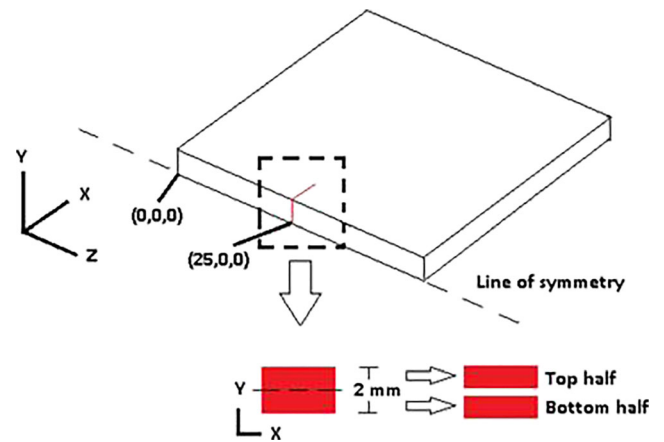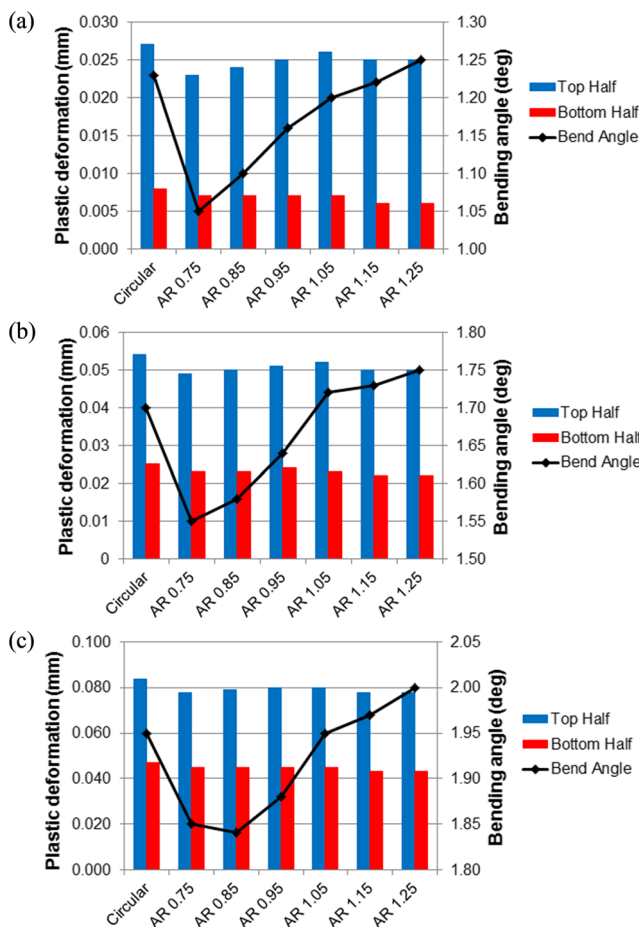

Fig. 9 Bending angle and plastic deformation of top and bottom halves of plate for different beam geometries at the plate centre at different laser power: **a** 400 W, **b** 600 W, **c** 800 W

Fig. 10 Area used in plastic deformation analysis

the highest bending angle amongst all beams. The area used to obtain the plastic deformation values is shown in Fig. 10.

Figure 11 shows the plastic strain distribution at the end of the cooling period for the triangular beam with the aspect ratios of 0.75, 1.05, and 1.25, measured at a cross-sectional area in the middle of the plate, as depicted in Fig. 10. This area is selected as it represents the typical plastic strain distribution along the heating path. From Fig. 11, it can be seen that the width (lateral direction) and the depth (thickness direction) of plastic strain distribution are highly influenced by the beam's lateral and longitudinal dimensions. Triangular beam with an aspect ratio of 1.25, which is the widest (7 mm) amongst all beams, produces lower but wider plastic distribution. The plastic strain distribution is also shallow in the top region of the plate. On the other hand, triangular beam with an aspect ratio of AR 0.75, which has the shortest lateral dimension (5.45 mm), produces a narrower plastic spread. Generally, the material under the scan spot shrinks in the x-axis (perpendicular angle to the laser beam movement direction) and expands in the thickness direction (y-axis). A small shrinkage also occurs in the z-direction (laser beam movement direction) which contributes to the edge effect.

4 Conclusion

This study has presented the effect of triangular laser beam with different aspect ratios in reducing edge effect in laser bending process. A finite element model was developed, and different sets of FE simulations were carried out by varying laser power value and constant scanning speed in order to understand the effect of beam geometries on final bending angle. From the analysis, triangular beam with a higher aspect ratio value tends to produce higher bending angle under the same laser power. This indicates that widening beam geometry has a more impact on the bending angle than lengthening it. As the laser power increases, the bending angle also increases. However, there is a threshold

Fig. 11 Plastic strain distribution for triangular beam with different aspect ratios: a AR 0.75, **b** AR 1.05, **c** AR 1.25, at a laser power of 400 W
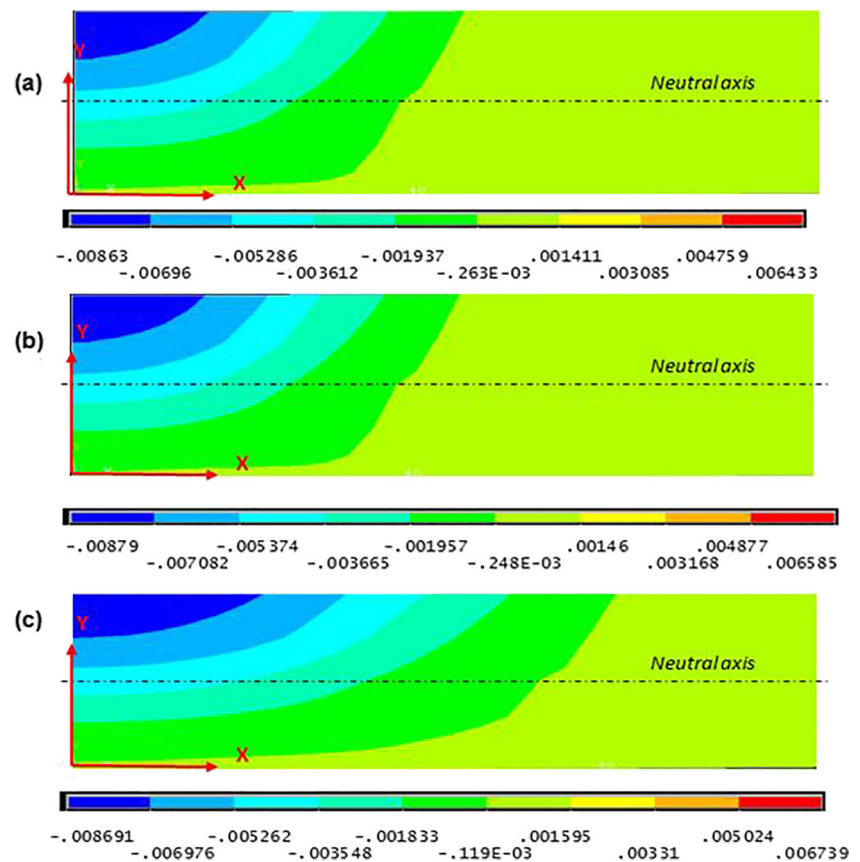
value for the aspect ratio value at 1.05, where the increment in bending angle started to level off even with the increasing value of aspect ratio. From the result gained, triangular beam is proved to be more effective in producing different ranges of bending angle value compared with circular beam with the same area of irradiation. It is significantly shown that triangular beams are more effective in minimizing the bending angle variation compared with the circular beam. Thus, the edge effect can be reduced as well by using triangular laser beam in laser forming process.

References

1. Jha GC, Nath K, Roy SK (2008) Study of edge effect and multi-curvature in laser bending of AISI 304 stainless steel. J Mater Process Technol 197:434–438. https://doi.org/10.1016/j.jmatprotec.2007.06.040
2. Shen H, Zhou J, Shi YJ, Yao ZQ, Hu J (2007) Varying velocity scan in laser forming of plates. Mater Sci Technol 23:483–486. https://doi.org/10.1179/174328407X179548
3. Safdar S, Li L, Sheikh MA, Liu Z (2007) Finite element simulation of laser tube bending: effect of scanning schemes on bending angle, distortions and stress distribution. Opt Laser Technol 39:1101–1110
4. Hu J, Cao Q, Shen H (2010) Experimental study on edge effects in laser bending. J Laser Appl 22:144–149
5. Birnbaum AJ, Cheng P, Yao YL (2007) Effects of clamping on the laser forming process. ASME J Manuf Sci Eng 129:1035–1044
6. Hu J, Xu H, Dang D (2013) Modeling and reducing edge effects in laser bending. J Mater Process Technol 213:1989–1996. https://doi.org/10.1016/j.jmatprotec.2013.05.007
7. Shi Y, Zhang C, Sun G, Li C (2016) Study on reducing edge effects by using assistant force in laser forming. J Mater Process Technol 227:169–177. https://doi.org/10.1016/j.jmatprotec.2015.08.018
8. Thomsen AN, Kristiansen E, Kristiansen M, Endelt B (2018) Influence of cooling on edge effects in laser forming. Procedia CIRP 74:394–397. https://doi.org/10.1016/j.procir.2018.08.155
9. Casamichele L, Quadrini F, Tagliaferri V (2007) Process-efficiency prediction in high power diode laser forming. J Manuf Sci Eng 129: 868. https://doi.org/10.1115/1.2738124
10. Chen ML, Jeswiet J, Bates PJ, Zak G (2008) Experimental study on sheet metal bending with medium-power diode laser. Proc Inst Mech Eng B J Eng Manuf 222:381–389. https://doi.org/10.1243/09544054JEM951
11. Cloots M, Uggowitzer PJ, Wegener K (2016) Investigations on the microstructure and crack formation of IN738LC samples processed by selective laser melting using Gaussian and doughnut profiles. Mater Des 89:770–784
12. Bielak R, Bammer F, Otto A, Stiglbrunner C, Colasse C, Murzin SP (2016) Simulation of forming processes with local heating of dual phase steels with use of laser beam shaping systems. Comput Opt 40:659–667

13. Safdar S (2007) Effects of non-conventional beam geometries in laser processing of engineering materials. PhD Thesis, The University of Manchester

14. Irawan P (2011) Study of the effects of laser beam geometries on laser bending of sheet metals. Master Thesis, The University of Manchester

15. Jamil MSC, Sheikh MA, Li L (2011) A study of the effect of laser beam geometries on laser bending of sheet metal by buckling mechanism. Opt Laser Technol 43:183–193. https://doi.org/10.1016/j.optlastec.2010.06.011

16. Kyriakongonas AP, Papazoglou VJ, Pantelis DI (2011) Complete investigation of austenitic stainless steel multi-pass welding. Ships Offshore Struct 6:127–144

17. Safdar S, Li L, Sheikh MA, Liu Z (2007) The effect of nonconventional laser beam geometries on stress distribution and distortions in laser bending of tubes. J Manuf Sci Eng 129:592. https://doi.org/10.1115/1.2716715

18. Shen H, Hu J, Yao Z (2010) Analysis and control of edge effects in laser bending. Opt Lasers Eng 48:305–315. https://doi.org/10.1016/j.optlaseng.2009.11.005

19. Jamil MSC, Fauzi ERI, Juinn CS, Sheikh MA (2015) Laser bending of pre-stressed thin-walled nickel micro-tubes. Opt Laser Technol 73:105–117